

$(e, e'\pi)$ reaction on light nuclei and spin-isospin strength distribution effects

Joseph Cohen and J. M. Eisenberg

Department of Physics and Astronomy, Tel Aviv University, Tel Aviv 69978, Israel

(Received 22 November 1982)

We study threshold pion electroproduction on light $T=0$ nuclei. The probe is especially interesting because it mixes longitudinal (spin component parallel to momentum transfer, $\vec{\sigma}\cdot\vec{k}$ coupling) and transverse ($\vec{\sigma}\times\vec{k}$ coupling) channels. Using the local density approximation for the treatment of possible nuclear spin-isospin mode enhancements, we calculate cross sections for both exclusive and inclusive measurements. For discrete nuclear levels we study differential cross sections of various pionlike levels, and these are compared with a nonpionlike excitation. The cross sections for exclusive excitations are extremely small except for forward angles. The inclusive cross sections, achieved by summing over all nuclear states, are considerably larger since these include the quasifree excitation. All cases are studied as a function of g' , the Migdal spin-isospin parameter. We find a strong influence of kinematical conditions (especially the energy transfer) and of nuclear density on enhancement phenomena.

NUCLEAR REACTIONS $^{16}\text{O}(e, e'\pi^-)^{16}\text{F}^*$, $^{16}\text{O}(e, e'\pi^-)X$; threshold
pion production cross sections for exclusive and inclusive measurements;
spin-isospin strength distribution effects.

I. INTRODUCTION

The reaction

$$A(J^P=0^+; T=0)(e, e'\pi) \\ \times A^*(J^P=0^-, 1^+, 2^-, \dots; T=1)$$

has been proposed¹ as a means of exciting the giant isovector odd-parity monopole resonance, and more recently² as a probe of spin-isospin effects and pion condensation precursor phenomena in nuclei. In view of recent experimental interest³ we were encouraged to carry out more detailed calculations of cross sections for this reaction. It seemed to us especially necessary to provide a more careful treatment of distortion of the pionic wave for the exclusive situation, and a fuller study of kinematics and limitations pertaining to the use of closure for the inclusive case. Furthermore, this kind of probe has the interesting theoretical feature of involving a mixture of both longitudinal ($\vec{\sigma}\cdot\vec{k}$, \vec{k} being the momentum transfer) and transverse ($\vec{\sigma}\times\vec{k}$) couplings.

Apart from the general interest in this process, the $(e, e'\pi)$ reaction, through its possible sensitivity to spin-isospin modes, may shed light on the problem of pion condensation precursor phenomena, discussed extensively in the last few years.⁴ Existing

evidence suggests that these phenomena are not seen strongly in nuclei, but it is desirable to look into the issue using various probes and kinematical conditions for the extensive mapping of nuclear spin-isospin strength. General aspects of the role of precursor phenomena in the softening of the quasielastic peak as seen by spin-isospin sensitive probes have been discussed by Alberico *et al.*⁵ Our earlier works^{2,10} and the present paper represent the realization of such conditions in the context of particular probes having spin-isospin character.

In this study we incorporate pion optical distortion and use the local density approximation (LDA) for the treatment of spin-isospin renormalization (Sec. II). We calculate cross sections for discrete levels (Sec. III) and for the inclusive case (Sec. IV). In Sec. V, we check the role of kinematical conditions in the general problem of precursor enhancement and pion condensation, as well as the influence of changes in the density parameters and the relative importance of the imaginary and delta-hole parts of the Lindhard function in the renormalization scheme for the transition operator.

II. FORMALISM

The $(e, e'\pi)$ reaction is governed at the threshold by the interaction²

$$H' = -\frac{ef}{m_\pi} \vec{\sigma} \cdot \vec{A} \vec{\tau} \cdot \vec{\varphi}, \quad (1)$$

where $e^2 \simeq 1/137$, $f^2/4\pi \simeq 0.08$, m_π and $\vec{\varphi}$ are the pion mass and isovector field, and $\vec{\tau}$ is the nucleon isospin matrix. In Eq. (1) \vec{A} is the Møller potential

$$\vec{A} = \frac{4\pi ie}{\vec{k}^2 - k_0^2} \bar{u}(\vec{p}') \vec{\gamma} u(\vec{p}) e^{i\vec{k} \cdot \vec{r}}, \quad (2)$$

with $u(\vec{p})$ and $u(\vec{p}')$ the electron spinors for incoming and outgoing momenta \vec{p} and \vec{p}' , and $\vec{k} = \vec{p} - \vec{p}'$, while $k_0 = p - p'$. The fivefold differential cross section for the pion electroproduction, where the pion is produced with momentum \vec{q} and energy ω_q and is scattered into the solid angle Ω_π while the outgoing electron is scattered into Ω_e' , is²

$$\frac{d^5\sigma}{d\Omega_e d\Omega_\pi d\omega_q} = \frac{q}{4(2\pi)^5} \frac{p'}{p} \left[\frac{4\pi e^2 f}{m_\pi} \right]^2 \frac{1}{(\vec{k}^2 - k_0^2)^2} \{ 2 \operatorname{Re}(\vec{p}' \cdot \vec{M}^*) (\vec{p} \cdot \vec{M}) - (\vec{M}^* \cdot \vec{M}) (\vec{p} \cdot \vec{p}' - pp') \}. \quad (3)$$

In Eq. (3),

$$\vec{M} = \left\langle f \left| \sum_{l=1}^A \{ \vec{\sigma} \tau_{\pm} e^{i\vec{k} \cdot \vec{r}} \varphi_{\vec{q}}^{(-)*}(\vec{r}) \}_l \right| i \right\rangle, \quad (4)$$

where $|i\rangle$ and $|f\rangle$ are the initial and final nuclear states, and $\varphi_{\vec{q}}^{(-)}(\vec{r})$ is the outgoing pionic wave. The electron waves are assumed to be plane waves, and we have used the extreme relativistic limit, $p, p' \gg m_e$; the operator τ_{\pm} refers to π^\mp production and in our convention $\tau_+ |n\rangle = \sqrt{2} |p\rangle$.

The effect of the nuclear medium on spin-isospin operators of the type appearing in Eq. (4) was shown⁶ to be a renormalization by means of the spin-isospin polarizability tensor

$$\begin{aligned} (\sigma_i \tau_\lambda)_{\text{ren}} &= \sum_{j=1}^3 \mu_{ij}(K, K_0) \sigma_i \tau_\lambda \\ &= \frac{\sigma_i \tau_\lambda}{1 + g' U(K, K_0)} - \frac{D_0(K, K_0) U(K, K_0)}{1 + W(K, K_0) U(K, K_0)} \frac{k_i \vec{\sigma} \cdot \vec{K} \tau_\lambda}{1 + g' U(K, K_0)}, \end{aligned} \quad (5)$$

where $K = |\vec{p} - \vec{p}' - \vec{q}| \approx k$ and $K_0 = p - p' - \omega = k_0 - \omega$, while

$$\mu_{ij}(K, K_0) = \frac{1}{1 + g' U(K, K_0)} \left[\delta_{ij} - K_i K_j \frac{D_0(K, K_0) U(K, K_0)}{1 + W(K, K_0) U(K, K_0)} \right]. \quad (6)$$

In Eqs. (5) and (6) we have the Lindhard function

$$U(K, K_0) = \frac{f^2(K^2)}{m_\pi^2} [U_N(K, K_0) + 4U_\Delta(K, K_0)], \quad (7)$$

and

$$W(K, K_0) = \frac{K^2}{K_0^2 - K^2 - m_\pi^2} + g', \quad (8)$$

where g' is the Migdal parameter,

$$D_0(K, K_0) = (K_0^2 - K^2 - m_\pi^2)^{-1} \quad (9)$$

is the pion free propagator, and

$$f^2(K^2) = f^2 \left[\frac{\Lambda^2 - m_\pi^2}{\Lambda^2 + K^2 - K_0^2} \right]^2 \quad (10)$$

is the coupling constant combined with the πNN

form factor, in which the cutoff is taken as $\Lambda = 1$ GeV. The Lindhard function contains a nucleon part and a delta-isobar part. The former is given by

$$U_N(K, K_0) = \frac{M^* p_F}{\pi^2} \left\{ 1 + \frac{p_F}{2K} [L(y_+) - L(y_-)] \right\}, \quad (11)$$

where the nucleon effective mass M^* is taken to be $0.8M_N$, with M_N the nucleon mass, and

$$L(y) = (1 - y^2) \log \left| \frac{1 + y}{1 - y} \right|, \quad (12)$$

$$y_{\pm} = \frac{M^* K_0}{p_F K} \pm \frac{K}{2p_F}. \quad (13)$$

The delta-isobar part of the Lindhard function is

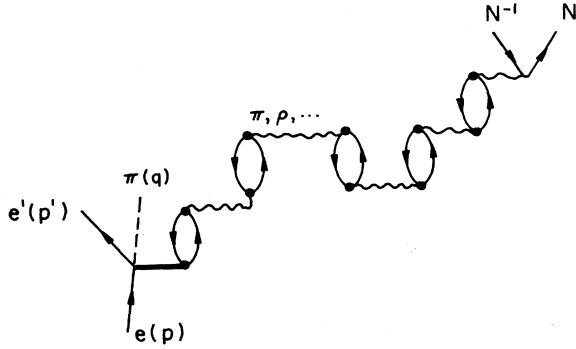


FIG. 1. Ring diagram summation for particle-hole renormalization of nuclear spin-isospin operators. The wavy line represents pion or ρ -meson exchanges or other short range correlations, while the bubbles represent $N^{-1}N$ and $N^{-1}\Delta$ configurations. We show the particular case treated here, in which the spin-isospin operator is supplied by the one-nucleon $eN \rightarrow e'\pi N$ amplitude.

$$U_{\Delta}(K, K_0) = \frac{8}{9} \frac{\omega_{\Delta}}{\omega_{\Delta}^2 - K_0^2} A \rho \quad (14)$$

for A nucleons in the Fermi gas model. In Eqs. (11)–(14) the Fermi momentum is denoted by p_F , ρ is the matter density normalized to unity, and $\omega_{\Delta} = 2.2m_{\pi}$.

We note that the Lindhard function develops an imaginary part for nonvanishing energy transfers K_0 , and these are studied in Sec. V. We also note that the renormalization of Eq. (5) mixes longitudinal and transverse spin components, unlike the situation for reaction mechanisms based purely on the longitudinal part.¹⁰

The physical picture behind this renormalization is the polarization of the nuclear medium through nucleon-hole and $\Delta(1232)$ -hole excitations. Iterations of all orders of particle-hole excitations, $N^{-1}N$ or $N^{-1}\Delta$, ring diagrams only, including π exchange as well as short-range correlations (ρ, ω, \dots , exchanges), result in the renormalization of Eq. (5). For the $(e, e'\pi)$ process the renormalization is shown in Fig. 1. The application of this renormalization in our calculation, which treats finite nuclei and not a nuclear medium, will be through an LDA. That is, we introduce $\rho(r)$ and $p_F[\rho(r)]$ in Eqs. (5)–(14), assuming that the nuclear density varies slowly enough so that it is meaningful at each radius r to

assign a local Fermi momentum, determined from the nuclear density at that radius, and then calculate the diamesic function as if given by the corresponding Fermi gas. This is not necessarily a very satisfactory approximation (and work is planned to replace it with a treatment appropriate to a finite system), but it does correctly weight the enhancement effects with the appropriately reduced density at the nuclear surface.

III. CALCULATIONS FOR DISCRETE NUCLEAR LEVELS

A. The scattering amplitude and local density approximation

We calculate the vector amplitude \vec{M} of Eq. (4) using the shell model. A nuclear level is characterized by a one-particle/one-hole (1p-1h) shell model configuration.⁷ Although the high momentum transfers involved do not allow the reliable use of the simple oscillator radial wave function $R_{nl}(r)$, we have exploited them for the exclusive case as a handy means for estimating cross sections. Since the resulting exclusive cross sections are much too small for experimental measurement, and the use of Eckart wave functions² does not change this conclusion, we saw no reason to improve the calculation from this point of view. On the other hand, from the theoretical side this exclusive calculation offers several interesting points for study, and also serves as a good starting point for treating inclusive cross sections.

We note that there is a small problem of double counting when a shell model approach is combined with the Lindhard function for nuclear matter in the LDA, since the nucleon part U_N includes overlap with the 1p-1h space of the discrete excitation. However, we anticipate no great problem from this source, since the main effects of the diamesic renormalization arise from very high-lying configurations well above the $0\hbar\omega$ or $1\hbar\omega$ excitations that we treat directly.

The differential cross section including renormalization of the transition operator is derived from Eqs. (3)–(5). These discrete nuclear excitations are all taken to be static ($K_0=0$). Introducing partial wave decomposition and carrying out the angular integration over the direction of \vec{r} , we have for numerical evaluation radial integrals of the form

$$\int_0^{\infty} dr R_{n_p l_p}(r) R_{n_h l_h}(r) u_{l_{\pi}}(qr) r j_{l_e}(kr) \frac{1}{1+g'U(K, K_0; r)} X(K, K_0; r), \quad (15)$$

TABLE I. Unenhanced cross section $d^3\sigma_0/d\omega_q d\Omega_{\vec{p}}$, (in units of $\mu\text{b}/\text{MeV sr}$) and enhancement factor R for discrete excitations in ^{16}O .

$J^P/\text{Configuration}$	p (MeV/c)	p' (MeV/c)	$d^3\sigma_0/d\omega_q d\Omega_{\vec{p}}$	$\theta_{\vec{p}'}=0.1$			$\theta_{\vec{p}'}=0.85$			
				$g'=0.40$	$g'=0.55$	$g'=0.70$	$g'=0.40$	$g'=0.55$	$g'=0.70$	
$0^-/(1p_{1/2})^{-1}2s_{1/2}$	400	230	1.2 (-2)	1.0	1.1	0.9	8.2 (-7)	13.2	2.8	1.4
	500	320	3.4 (-3)	0.5	1.0	1.0	4.4 (-7)	11.2	3.4	1.8
	600	380	5.1 (-3)	11.5	2.5	1.1	2.1 (-7)	11.3	4.4	2.3
	800	580	3.2 (-3)	12.0	2.5	1.1	1.1 (-9)	6.6	4.2	2.8
$1^-/(1p_{1/2})^{-1}2s_{1/2}$	400	230	1.9 (-3)				2.8 (-6)			
	500	320	4.3 (-3)				2.6 (-6)			
	600	380	8.3 (-3)				1.9 (-6)			
	800	580	4.3 (-3)				3.2 (-8)			
$2^-/(1p_{1/2})^{-1}2d_{5/2}$	400	230	2.0 (-1)	2.2	1.2	0.7	2.1 (-6)	3.2	0.5	0.2
	500	320	1.3 (-1)	2.6	1.3	0.8	1.7 (-7)	0.7	0.9	1.1
	600	380	9.6 (-2)	4.5	1.8	1.0	1.6 (-7)	3.3	1.2	1.0
	800	580	5.0 (-2)	4.7	1.8	1.0	5.4 (-9)	1.6	1.1	0.8

where X may be either 1 or

$$U(K, K_0; r) / [1 + W(K, K_0)U(K, K_0; r)]$$

[see Eq. (5)], and depends on r through $p_F(\rho)$ and $\rho(r)$. In Eq. (15) the subscripts h and p refer to the hole and particle states, l_π and l_e are orbital angular momenta of the pion (momentum \vec{q}) and electron (momentum \vec{k}) partial waves. These last were taken as spherical Bessel functions $j_{l_e}(kr)$ for the electrons and distorted waves $r^{-1}u_{l_\pi}(qr)$ for the pion. In this radial integral we now use the LDA in the Lindhard function U , that is, we introduce $U\{p_F[\rho(r)]\}$ in terms of the quantities of Eqs. (7), (11), and (14), recalling

$$p_F(\rho) = \left[\frac{3}{2} \pi^2 A \rho(r) \right]^{1/3}. \quad (16)$$

The density $\rho(r)$ was taken in the Fermi form

$$\rho(r) = \frac{3}{4\pi c^3} \left\{ (1 + \pi^2 t^2 / c^2) \left[1 + \exp \left(\frac{r-c}{t} \right) \right] \right\}^{-1}, \quad (17)$$

where c denotes the nuclear half-density radius, and $a = 4.40t$ is the nuclear surface thickness.

The pionic waves were distorted by using subroutines from the computer code DWPI,⁸ modified by us to include true absorption with the optical potential of Stricker *et al.*⁹ Details are given in Ref. 10.

B. Estimates of exclusive cross sections

Calculations were carried out for ^{16}O and for ^{12}C . For ^{16}O the parameters chosen were $c = 2.6$ fm and $a = 2.3$ fm,¹¹ while for ^{12}C we have $c = 2.3$ fm.¹¹ The calculations were carried out mainly for

$$(Z, N)(e, e'\pi^-)(Z+1, N-1),$$

for which the cross section is three to four times higher than for $(e, e'\pi^+)$. Detailed results were obtained for $p = 400, 500, 600,$ and 800 MeV/c, with p' ranging between its value at the pion threshold and downwards by about 100 MeV/c. The resulting cross sections were, in all cases, very small, excluding very forward outgoing electron angles ($\theta_{p'} \lesssim 10^\circ$), where they are higher. The decrease of the cross section with $\theta_{p'}$ is very rapid. Table I shows the discrete unenhanced cross sections for ^{16}O along with enhancement factors $R \equiv d^3\sigma_{\text{ren}}/d^3\sigma_0$ (i.e., the differential cross section integrated over the outgoing pion angles with the renormalized operator divided by the same cross section without renormalization) for $g' = 0.40, 0.55,$ and 0.70 . Similar calculations for the $J^P = 1^+, T = 1$ level in ^{12}C [using the pure configuration $(1p_{3/2})^{-1}1p_{1/2}$ because of com-

putational difficulties although our formalism allows for configuration mixing] gave similar results.

In addition to the immediate realization that such small exclusive cross sections would not enable any significant experimental measurement at present, we can make several observations from Table I, as well as from results not quoted here in detail:

(a) For the low-lying ^{16}O levels (appearing first in the table), we note that the nonpionlike level $J^P = 1^-$ is not suppressed with respect to the pionic ones $J^P = 0^-$ and 2^- except, possibly, for a very low energy pion. [Even this last suppression disappears for pions of kinetic energy ≥ 10 MeV. We also note that to get this suppression the incoming electron must not be too energetic ($p \lesssim 500$ MeV/c).] The $J^P = 3^-$ level is strongly suppressed under these conditions, but equals the 2^- level for the 800 MeV/c incoming electron.

(b) In the high-lying group of levels ($J^P = 0^-, 1^-, 2^-$) one fails to observe any suppression of the 1^- level compared to the pionlike pair ($0^-, 2^-$). It seems that this probe does not provide a clear selection of pionlike levels over and above other levels, as was the case with the $(\pi, 2\pi)$ reaction.¹⁰ This is, of course, related to the above-mentioned mixture of transverse and longitudinal channels.

(c) It is interesting to note in Table I that some conditions lead to R less than unity. This can occur here because of the admixture of significant transverse $\vec{\sigma} \times \vec{k}$ components which are suppressed rather than enhanced by pionic effects.

(d) The enhancement factor presented in Table I is very large in the region of the critical momentum, as is to be expected. It is similar for the two reactions $(e, e'\pi^\pm)$.

We also investigated the importance of pion distortion in the calculation. Towards this end, we first compared cross sections for plane waves (Coulomb distortion only), nuclear optical potential distortion (no Coulomb) only, and full distortion.

We find that the nuclear optical potential has the most important effect on the cross section, even though the pion is quite low in energy; the Coulomb distortion has a much smaller effect than the nuclear optical potential in determining the difference between plane-wave and fully-distorted-wave results. We further studied the relative importance of optical distortion and true absorption. Towards this end we calculated the cross section for nuclear optical distortion only ($B_0 = C_0 = 0$ for true absorption parameters) compared with true absorption only (only $B_0, C_0 \neq 0$). The cross sections indicate that the two parts of the optical potential are equally important: The optical and true absorption should both be included in distorting such low-energy pions. Since the exclusive cross sections are very small (several orders of magnitude below the required magnitude for experimental measurements) we turn now to the inclusive case.

IV. INCLUSIVE CALCULATIONS FOR PLANE WAVES IN THE LDA

A. Formalism, closure approximation, inclusive cross section, and LDA

In a previous work¹⁰ we found that for momentum transfer above 300 to 400 MeV/c it is possible to apply the closure approximation very reliably in summing over nuclear states. Using this, we sum over final states $|f\rangle$ in the expression for the exclusive cross section and find a single-nucleon and a two-nucleon contribution. Here, we analyze the one-body part, dropping the spin-isospin correlation term, which is expected to be small. Choosing spin-saturated nuclei, and studying plane-wave pions (as explained later, we do not expect large effects from distortion) we find for the inclusive cross section, after renormalizing the operator and applying the local density approximation,

$$\sum_f \frac{d^5\sigma}{d\Omega_p d\Omega_q d\omega_q} = \frac{q}{4\pi^3} \frac{p'}{p} \frac{e^4 f^2}{m_\pi^2} \frac{1}{(\vec{k}^2 - k_0^2)^2} \frac{A}{2} \left[a_1 \int_0^\infty \eta(r) dr - 2a_2 \int_0^\infty \eta(r) \xi(r) dr + a_2 K^2 D_0(K, K_0) \right. \\ \left. \times \int_0^\infty \eta(r) \xi^2(r) dr \right], \quad (18)$$

where

$$a_1 = 3pp' - \vec{p} \cdot \vec{p}', \quad (19a)$$

$$a_2 = [2(\vec{p} \cdot \vec{K})(\vec{p}' \cdot \vec{K}) + (pp' - \vec{p} \cdot \vec{p}')K^2] D_0(K, K_0), \quad (19b)$$

and

$$\eta(r) = 4\pi r^2 \frac{\rho(r)}{[1 + g'U(K, K_0; r)]^2}, \quad (20a)$$

$$\xi(r) = \frac{U(K, K_0; r)}{1 + W(K, K_0)U(K, K_0; r)}. \quad (20b)$$

TABLE II. Enhancement factor R_{inc} for inclusive ($e, e'\pi$) and differing values of k , g' , and $\theta_{\vec{p}'}$.

Nucleus	p^a	k^a	$\theta_{\vec{p}'}=7.5^\circ$			$\theta_{\vec{p}'}=18.1^\circ$				$\theta_{\vec{p}'}=28.8^\circ$				
			$g'=0.40$	$g'=0.55$	$g'=0.70$	k	$g'=0.40$	$g'=0.55$	$g'=0.70$	k	$g'=0.40$	$g'=0.55$	$g'=0.70$	
^{16}O	400	179	1.53	1.11	0.90									
		203	1.66	1.21	0.98	219	1.51	1.15	0.95	244	1.32	1.05	0.89	
		252	1.68	1.32	1.09	262	1.59	1.26	1.05	278	1.46	1.17	1.00	
	800	220	1.54	1.17	0.97									
		242	1.57	1.23	1.02	310	1.26	1.05	0.90					
		265	1.62	1.28	1.07	326	1.32	1.10	0.96					
		311	1.77	1.40	1.16	360	1.43	1.19	1.03	434	1.21	1.04	0.91	
	^{12}C	400	179	1.15	0.91	0.78								
			203	1.44	1.15	0.98	219	1.35	1.11	0.95	244	1.23	1.03	0.90
228			1.48	1.21	1.03	240	1.41	1.16	1.00	261	1.29	1.08	0.94	
252			1.52	1.25	1.08	262	1.45	1.21	1.04	278	1.35	1.13	1.00	
800		220	1.37	1.12	0.97									
		242	1.42	1.18	1.01	310	1.28	1.10	0.96					

^aAll momenta (p, k) are given in units of MeV/c.

In treating the physical aspects of the inclusive reaction within the closure approximation, one should define an average nuclear excitation $\bar{\epsilon}$ [in the spirit of Sec. III, this is the equivalent level which, when used in Eq. (18), gives the same result that would have been obtained by summing explicitly over the various discrete nuclear levels]. Adopting the view that the quasifree peak constitutes the main contribution to the cross section,¹⁰ we take, after averaging over outgoing pion angles,

$$\bar{\epsilon} = \frac{k^2}{2M_N} \quad (21)$$

B. Results for plane waves

Checks of cross section sensitivity to kinematical variables showed that the dependence upon the azimuthal angle of the pion, $\phi_{\vec{q}}$, is negligible even for pions with energy up to $0.5m_\pi$. The change of the same quantity with $\theta_{\vec{q}}$ is moderate, and amounts to about 10% over the range 0 to π radians. Calculations based on Eq. (18) were carried out (with the integrals calculated numerically) for various values of $\theta_{\vec{q}}$ and $\theta_{\vec{p}'}$, followed by summation over $\Omega_{\vec{q}}$. It was found that the cross section falls rapidly with $\theta_{\vec{p}'}$, and from 6° to 60° it loses four orders of magnitude. Thus, differential cross sections were calculated for $\theta_{\vec{p}'}$ in the range 7.5° – 50° divided into four equal intervals ($\theta_{\vec{p}'}=7.5^\circ, 18.1^\circ, 28.8^\circ, 39.4^\circ$, and 50°) with no integration over $\theta_{\vec{p}'}$ (because of the ra-

pid fall in cross section). Calculations were carried out for $p=400, 500$, and 800 MeV/c for ^{16}O and for a few threshold cases for ^{12}C at $p=800$ and 400 MeV/c [again using¹¹ $c=2.6$ fm and $a=2.3$ fm for the density of ^{16}O , and $c=2.3$ fm and $a=2.3$ fm for ^{12}C].

In Table II we show the enhancement factor $R_{\text{inc}}=d^3\sigma_{\text{ren}}/d^3\sigma_0$ for the inclusive case for various values of k and $\theta_{\vec{p}'}$, and for g' in the range 0.4–0.7. It is easily seen that R_{inc} rises slowly in approaching the critical momentum $k\sim 2-3m_\pi$, but is not strongly dependent on g' ; its dependence on k is also not strong. This will not allow for the conclusive detection of spin-isospin effects with this reaction, at least for the relatively large energy transfer involved in the quasifree excitation. Figure 2 gives the characteristic behavior of $d^3\sigma_0/d\Omega_{\vec{p}'}d\omega_q$ as a function of k . Similar results were obtained for $p=500$ MeV/c (and are not quoted here). The differences in enhancement factors R_{inc} for similar k values come about because in Eqs. (18)–(20) we have two different types of kinematical factors and integrals (a_1 and a_2 ; η and ξ). Although the integrals depend exclusively on the magnitude of k (and quite weakly so, in fact), the kinematical factors show strong dependence on the direction of \vec{k} , determined by the vectors \vec{p} and \vec{p}' . In R_{inc} there enters a_1/a_2 , among other ratios, and thus the combination of kinematics with the mixing of spin components through the polarizability tensor μ_{ij} , Eq. (5), results in the dependence of R_{inc} on $\theta_{\vec{p}'}$ in Table II. We found that the renormalization through μ_{ij} causes

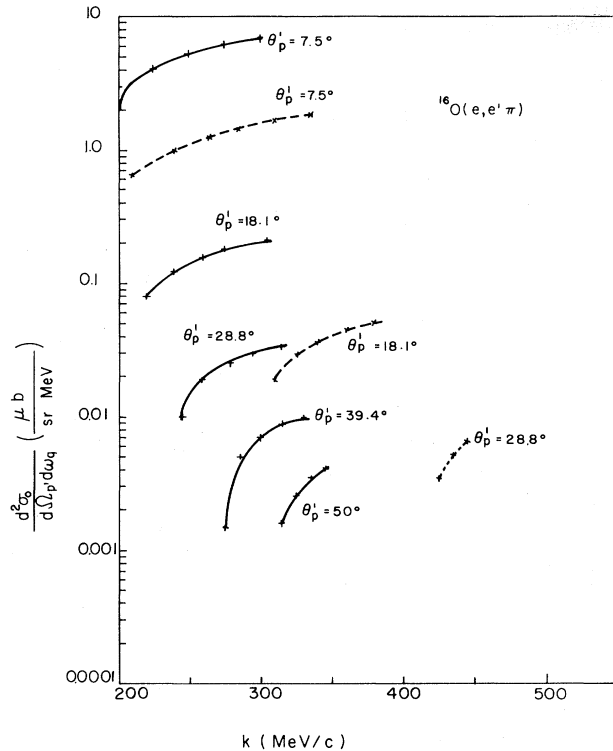


FIG. 2. Unrenormalized plane-wave inclusive differential cross section $d^2\sigma_0/d\Omega_{\vec{p}}d\omega_q$ as a function of momentum transfer k . Dashed lines refer to $p=800$ MeV/c while full ones to 400 MeV/c, and the parameter $\theta_{\vec{p}'}$ indicated in the graphs is the outgoing electron angle.

the main sensitivity to $\theta_{\vec{p}'}$, and that the second term of this tensor is responsible for the main part of the enhancement. We again note the existence of regions with $R < 1$ for high g' values, resulting from transverse $\vec{\sigma} \times \vec{k}$ components and the larger region of repulsive force for these cases.

It is clear that the effects of pionic distortions reported in this section will have no great impact on our inclusive results. We recall,¹⁰ in particular, that for the inclusive case no optical distortions are to be included, and thus the effect of partial distortions arising from true absorption would be a reduction in cross section and, because of the enhancement of low nuclear density, a further approach of R_{inc} to unity.

V. DISCUSSION AND CONCLUSIONS

Let us first clarify what it is that makes the inclusive $(e, e'\pi)$ reaction relatively insensitive to spin-isospin correlation effects. We start with the influence of kinematical conditions governing the reaction, especially the energy transfer. As already pointed out by Ericson and Delorme,⁴ the spin-isospin strength distribution effects are strong for vanishing energy transfer with momentum transfer in the critical region $k \sim 2-3m_\pi$. To check this point, we force $K_0=0$ in Eqs. (19) and (20) (there is no energy transfer to the nucleus even though we anticipate dominant excitation of the quasifree peak). We then found large changes in the enhancement factor for low g' with the momentum transfer around $k \approx 2-3m_\pi$, as shown in Table III.

We also checked the importance of the imaginary part of the Lindhard function¹² in the renormalization of the operator [Eq. (5)]. In our case $\text{Im}U_\Delta=0$, since our energy transfer is in any event below pion production threshold. Inserting $\text{Im}U$ into Eq. (5) we found a small effect, of less than 5% for $g'=0.40$, of 2-3% for $g'=0.55$, and $\leq 1\%$ for $g'=0.70$.

Turning to the nuclear density, we found an interesting effect arising from changing the density parameters of ^{16}O by taking $a=1.8$ fm (instead of 2.3 fm) and $c=2.4$ fm (instead of 2.6 fm) which implies a central nuclear density of $\rho_0=0.21$ fm⁻³.

TABLE III. Enhancement factor R_{inc} , but with zero energy transfer to the nucleus, for the reaction $^{16}\text{O}(e, e'\pi)$.

p^a	k^a	$\theta_{\vec{p}'}=7.5^\circ$			k	$\theta_{\vec{p}'}=18.1^\circ$			k	$\theta_{\vec{p}'}=28.8^\circ$		
		$g'=0.40$	$g'=0.55$	$g'=0.70$		$g'=0.40$	$g'=0.55$	$g'=0.70$		$g'=0.40$	$g'=0.55$	$g'=0.70$
400	203	3.70	1.54	0.92	219	3.89	1.50	0.88	244	4.09	1.41	0.82
	228	5.22	1.87	1.06	240	5.31	1.79	1.01	261	5.29	1.66	0.94
	252	6.99	2.17	1.19	262	6.89	2.07	1.14	278	6.59	1.90	1.05
800	220	4.05	1.55	0.91								
	242	5.56	1.86	1.04	310	5.20	1.56	0.91				
	265	7.21	2.14	1.17	326	5.66	1.71	0.99				
	288	8.50	2.35	1.27	343	5.72	1.82	1.06	423	2.12	1.16	0.83
	311	9.11	2.50	1.35	360	5.54	1.90	1.11	434	2.14	1.22	0.89

^aAll momenta (p, k) are given in units of MeV/c.

TABLE IV. Enhancement factor R_{inc} , but with smaller density parameters ($a = 1.8$ fm and $c = 2.4$ fm) for the reaction $^{16}\text{O}(e, e'\pi)$.

p^a	k^a	$\theta_{p'} = 7.5^\circ$			k	$\theta_{p'} = 18.1^\circ$		
		$g' = 0.40$	$g' = 0.55$	$g' = 0.70$		$g' = 0.40$	$g' = 0.55$	$g' = 0.70$
800	220	2.66	1.48	0.96	310	1.69	1.22	0.93
	242	2.84	1.64	1.08				

^aAll momenta (p, k) are given in units of MeV/ c .

Although no significant changes are seen in the inclusive cross sections for $g' = 0.70$, those for $g' = 0.40$ are higher by 50–80%, as shown in Table IV (including $\text{Im}U$). These results are easily understood if we note that with the new parameters the nuclear radius, as well as the surface thickness, are smaller, thus raising the effective matter density and accentuating the pion-condensation effects. Note that this is the source of the numerical differences between our results and those of Ref. 2, since our parameters¹¹ are slightly different from the ones used there.

Lastly, we note the results of checking the relative importance of U_Δ in the renormalization. Suppression of U_Δ , so that the renormalization stems from the nucleon-hole contribution, results in an enhancement factor R_{inc} which is almost k independent, and varies slowly with \bar{p} , $\theta_{\bar{p}}$, and g' (see Table V).

Our present results are in agreement with those of Alberico *et al.*⁵ whose quasifree peak is enhanced by a factor of 2 for $g' = 0.60$ and by 1.5 for $g' = 0.70$. Their results are obtained for constant central density ρ_0 and for constant Fermi momentum $p_F = 1.36$ fm⁻¹, while for the parameters used here almost all the nucleons are at the nuclear surface.

We conclude that the inclusive cross section for

$(e, e'\pi)$ exhibits sensitivity of 10–40% to spin-isospin strength distribution effects for the range of g' we have considered. We note, in particular, that the great sensitivity to kinematical conditions emphasizes the need for very accurate and detailed measurements in all questions of enhancements resulting from spin-isospin strength distribution and of possible pion condensation precursors. We have considered here the parameter g' in the range $0.4 \leq g' \leq 0.7$, which roughly spans the region from actual pion condensation at central nuclear densities to minimal condensation effects.⁴ We recall that the currently accepted value is $g' \simeq 0.7$; we do not show results for g' above this value since there the effects on the spin-isospin strength tend to be even less than 10%. Thus the inclusive process, because of its large energy transfer, is not apt to be highly useful for the study of such effects. On the other hand, the $(e, e'\pi)$ excitation of discrete levels exhibits large changes (by as much as an order of magnitude in some cases) with the inclusion of spin-isospin renormalization; however, cross sections to these levels are very small. Nonetheless, the consideration of spin-isospin strength distributions will be important for quantitative work with the pion electroproduction reaction.

TABLE V. Enhancement factor R_{inc} , but with Δ -hole contribution suppressed, for the reaction $(e, e'\pi)$.

Nucleus	p^a	k^a	$\theta_{\bar{p}} = 7.5^\circ$			k	$\theta_{\bar{p}} = 18.1^\circ$		
			$g' = 0.40$	$g' = 0.55$	$g' = 0.70$		$g' = 0.40$	$g' = 0.55$	$g' = 0.70$
^{16}O	400	179	1.25	1.06	0.94	219	1.18	1.05	0.96
		203	1.27	1.11	0.99				
	800	220	1.19	1.06	0.97	310	1.05	0.99	0.93
		242	1.18	1.08	1.00				
		335	1.22	1.13	1.06				
	^{12}C	400	179	1.20			240	1.14	
228			1.18						
800		220	1.15			310	1.04		
		242	1.15						

^aAll momenta (p, k) are given in units of MeV/ c .

ACKNOWLEDGMENTS

M. Ericson and T. E. O. Ericson are warmly thanked for fruitful discussions and kind hospitality during a short stay by one of us (J.C.) at CERN. J. Lichtenstadt is thanked for interesting comments

concerning the experimental aspects of this work and W. M. Alberico for enlightening discussions on theoretical features. This research was supported in part by the U.S.-Israel Binational Science Foundation and by the Israel Academy of Sciences and Humanities—Basic Research Foundation.

-
- ¹J. M. Eisenberg and H. J. Weber, *Phys. Lett.* **34B**, 107 (1971).
²J. M. Eisenberg, *Nucl. Phys.* **A355**, 312 (1981).
³J. Lichtenstadt, private communication; B. Saghai, private communication.
⁴M. Ericson and J. Delorme, *Phys. Lett.* **76B**, 182 (1978); J. Meyer-ter-Vehn, *Phys. Rep.* **74**, 323 (1981); W. Weise, *Nucl. Phys.* **A374**, 505C (1982); J. Delorme, *ibid.* **A374**, 541C (1982); E. Oset, H. Toki, and W. Weise, *Phys. Rep.* **83**, 281 (1982).
⁵W. M. Alberico, M. Ericson, and A. Molinari, in contributed papers for the International Conference on High Energy Physics and Nuclear Structure, Versailles, 1981 (unpublished); W. M. Alberico, M. Ericson, and A. Molinari, *Phys. Lett.* **92B**, 153 (1980); *Nucl. Phys.* **A379**, 429 (1982).
⁶N. C. Mukhopadhyay, H. Toki, and W. Weise, *Phys. Lett.* **84B**, 35 (1979).
⁷J. M. Eisenberg and W. Greiner, *Microscopic Theory of the Nucleus* (North-Holland, Amsterdam, 1972).
⁸R. A. Eisenstein and G. A. Miller, *Comput. Phys. Commun.* **11**, 96 (1976).
⁹K. Stricker, H. McManus, and J. A. Carr, *Phys. Rev. C* **19**, 929 (1979).
¹⁰J. Cohen and J. M. Eisenberg, *Nucl. Phys.* **A395**, 389 (1983).
¹¹C. W. de Jager *et al.*, *At. Data Nucl. Data Tables* **14**, 489 (1974).
¹²A. L. Fetter and J. D. Walecka, *Quantum Theory of Many Particle Systems* (McGraw-Hill, New York, 1971), pp. 151–197.